ELSEVIER

PII: S0144-8617(96)00074-4

*Carbohydrate Polymers* **30** (1996) 149–153

0144-8617/96/$15.00 + .00

# Sol–gel transition of polysaccharide gellan gum

**T. Okamoto & K. Kubota**

*Department of Biological and Chemical Engineering, Faculty of Technology, Gunma University, Kiryu, Gunma 376, Japan*

The gelation of an extracellular polysaccharide gellan gum was investigated by the dynamic and static light scattering technique focusing on the sol–gel transition. The gel point was determined by the qualitative change of profiles of the correlation functions. The mass and correlation length for the growing clusters were evaluated by the angular dependence of the scattered light with the sample cell being rotated. The degree of gelation characterizing sol–gel transition was obtained from the elapsed time after a temperature quench for starting the gelation. The critical exponents $\gamma$ and $\nu$ corresponding to the cluster mass and correlation length, respectively, were obtained as 1.66 and 0.88. The resultant critical exponents are in good agreement with the three-dimensional percolation model. Copyright © 1996 Elsevier Science Ltd

## INTRODUCTION

Gels have attracted much attention in various fields because of their possible unique applications, and investigations related to gels have been developed in recent years. Many polysaccharides have the ability to form gels and they have been used especially in the field of food for a long time. Gelation is identified as a macroscopic network formation and the gel structure is affected essentially by the gelling process. To clarify the gelling mechanism based on the chemical nature has become more and more important.

Gellan gum is an extracellular microbial polysaccharide from *Pseudomonas eoldea*, and forms a firm and very transparent gel in the presence of metallic ions. The chemical structure of gellan has been confirmed as a linear anionic heteropolysaccharide consisting of glucose, glucuronic acid, glucose and rhamnose as a repeating unit (Milas *et al.*, 1990). It is a characteristic feature to have a carboxyl unit in a repeating unit and the interaction of this unit with divalent ions, e.g. $Ca^{2+}$ ion, acts as a junction zone (eggbox structure) to form the gel. It has been reported that gellan shows a structural (conformational) change from the disordered state (single strand) to the ordered state (double strand) (Dentini *et al.*, 1988; Denkinger *et al.*, 1989). Gellan molecules in the ordered state have a relatively stiff structure and the detailed characterization of the molecular structure has been reported before (Okamoto *et al.*, 1993). In the ordered state, the molecular weight is $23.8 \times 10^4$, having a double helical conformation, and gellan molecules are fairly stiff, characterized by the persistence length of 98 nm. The radius of gyration is about 100 nm, and the gellan molecules entangle with each other even at a concentration as low as 0.1%. This entanglement will work effectively in the gelling process.

The general model of gelation or sol–gel transition is the percolation theory (Stauffer *et al.*, 1982; Stauffer, 1985). In the percolation theory various quantities characterizing the gelation process such as cluster mass and size can be expressed by the power–law relations against the degree of gelation $\varepsilon$. $\varepsilon$ is defined as $\varepsilon = 1 - p/p_c$ with $p(p_c)$ being the (critical) crosslinking probability. In the case that the reaction of network formation is sufficiently slow and is presumed to proceed linearly with time, $\varepsilon$ can be equated to $1 - t/t_g$ with $t$ and $t_g$ being the elapsed time and the gelation time. The essential features of the gelling mechanism can be characterized from such power–law relations. For example, site-percolation for a two-dimensional square lattice shows that a macroscopic cluster is formed when the site occupation probability is 0.59 and more. This value of 0.59 is the critical site fraction probability for the percolation. Such a process corresponds to the sol–gel transition and such a critical point is regarded as a gel point.

It has been shown by dynamic light scattering studies that the profile of the normalized net intensity correlation function $g^{(2)}(\tau)$ changes behavior from a stretched exponential form to a power–law form ($g^{(2)}(\tau) \sim \tau^{-2\phi}$) against time as the gel point is approached (Martin & Wilcoxon, 1988). For a semidilute solution of polyurethane clusters, exponents $\phi = 0.23$–$0.38$ have been reported (Adam *et al.*, 1988). Lang & Burchard (1991)

obtained for tamarind gum that the electric field correlation function $g^{(1)}(\tau)$ shows a power-law form with the exponent $\phi = 0.34$ at the gel point (Lang & Burchard, 1991). Power-law form is a good measure of gel point and it is possible to determine the gel point *in situ* by the profile change of correlation function simultaneously with scattering intensity measurements.

In the present report we studied the sol–gel transition of aqueous gellan solution in the presence of $Ca^{2+}$ ions, based on the percolation model using dynamic and static light scattering measurements. Gellan is suitable for light scattering measurement because of the formation of very transparent gel.

## EXPERIMENTAL

### Sample preparation

Gellan gum was kindly supplied from San-Ei-Gen F.F.I. Ltd. The original sample (Lot No. 62058A) was further purified and converted to tetramethylammonium-type in order to avoid aggregation (Okamoto *et al.*, 1993). The purified gellan was first dissolved in pure water and the solution was heated at about 90°C for 4 h.Then, the solution was mixed with hot $CaCl_2$ aqueous solution to adjust the final concentration at about 50°C. Mixed sample solution was filtered directly into the optical cell through a 0.45 μm nylon filter. Special care to avoid the temperature decrease of the sample solution was paid in these procedures. After thorough equilibrium was achieved, the temperature was decreased slowly and was held at about 35°C for a while. In this condition, gellan molecules take a double helical structure with sufficient molecular dispersion. Then, the sample solution was quenched to the final temperature. The elapsed time was started to be counted and light scattering measurements were carried out successively as a function of elapsed time.

### Light scattering

The light scattering measurements were carried out using a homemade spectrometer. Figure 1 shows the schematic diagram. The light source was an Ar ion laser operated at 488 nm. The optical cell was rotated at 6 rpm to keep the isotropic (ergodic) condition near the gel point. Two types of homemade correlators were used for the correlation function measurements. One is a single-clipped 256 channel linear correlator and the other was a multi-tau 4-bit correlator covering 5.3 decades of delay time. In the case of linear correlator, the correlation functions were collected over an extensive delay time by changing the sample time and by data merging (superposing) method. The temperature of the sample solution was regulated within 0.01°C.

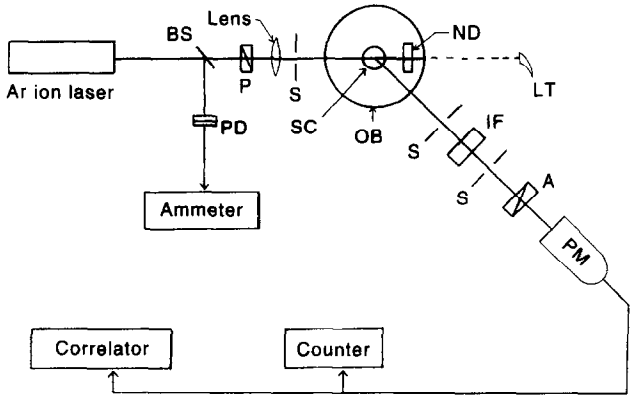


**Fig. 1.** Schematic diagram of homemade light scattering apparatus. BS: beam splitter; P: polarizer; S: slit; PD: photodiode; SC: sample cell; OB: oil bath; ND: neutral density filter; LT: light trap; IF: interference filter; A: analyser; PM: photomultiplier tube. Sample cell in the temperature regulated oil bath was rotated in case of scattering intensity measurements.

## RESULTS AND DISCUSSION

We first examined the qualitative characteristics of the profiles of correlation functions at the equilibrium state. Figure 2 shows the double logarithmic plot of the normalized correlation function, $g^{(1)}_{app}(\tau)$, for 0.1% gellan gum at various $Ca^{2+}$ concentrations, and various temperatures. Here we plotted apparent normalized electric field correlation function, defined as $g^{(1)}_{app}(\tau) = [(G^{(2)}(\tau)-\text{Base})/(G^{(2)}(0)-\text{Base})]^{1/2}$ $(= g^{(2)}(\tau)^{1/2})$ with $G^{(2)}(\tau)$ being the intensity autocorrelation function. The subscript app means that $[(G^{(2)}(\tau)-\text{Base})/(G^{(2)}(0)-\text{Base})]^{1/2}$ is not necessarily equal to the dynamic structure factor under the restriction of ergodic condition (possible difference between time average and ensemble average) at the gel state (Pusey & Megen, 1989; Joosten *et al.*, 1991; Xue *et al.*, 1992), and we used this $g^{(1)}_{app}(\tau)$ only for the indication of the characteristic profile of correlation function and for the decision of the gel point. Figure 2(a) shows the temperature dependence of 0.1% gellan gum at equilibrium state set at respective temperature for three days. The samples at 43 and 37°C were in the sol state which showed a distinct fluidity. On the other hand, the sample at 32°C formed a weak gel and the sample at 27°C formed a fairly hard gel. The functional shapes at 43 and 37°C are convex upwards as in the usual isotropic polymer solutions, and those at 32 and 27°C are convex downwards and have long tails at large delay time. The appearance of a long tail in $g^{(1)}_{app}(\tau)$ suggests that the gel of gellan gum is fairly homogeneous and the effect of nonergodicity observed in the chemical gel (e.g. polyacrylamide gel) is not large in the present correlation function measurement conditions (Joosten *et al.*, 1991). Figure 2(b) shows correlation functions at various $Ca^{2+}$ ion concentrations and various temperatures in the equilibrium state. The curve *c* is remarkable and shows a

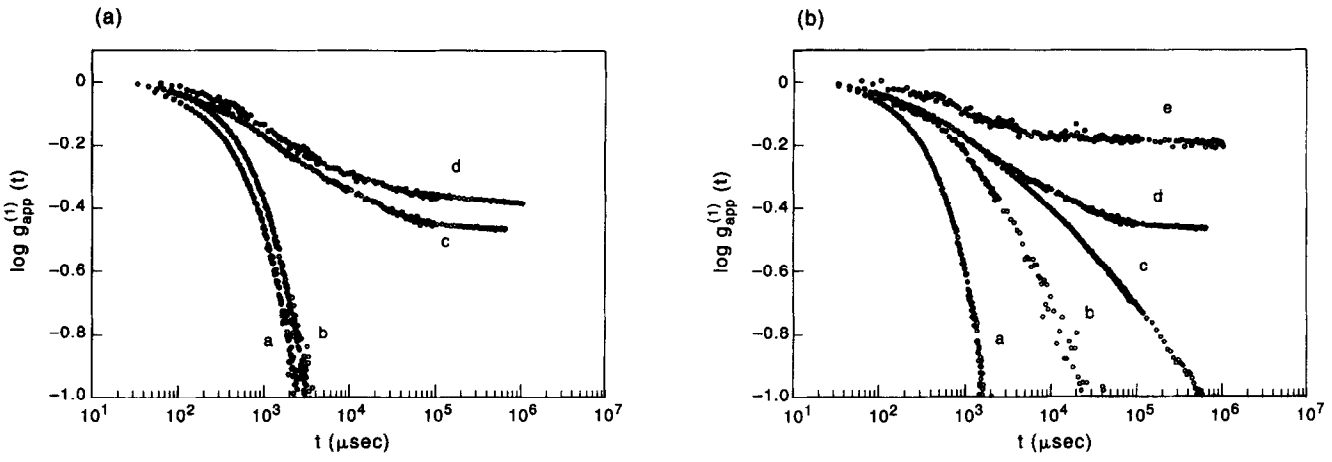


**Fig. 2.** (a) Time correlation function, $g^{(1)}{}_{app}(\tau)$ for 0.1% gellan gum in 3 mM $Ca^{2+}$ at (a) 43, (b) 37, (c) 32, and (d) 27°C. (b) Time correlation function for 0.1% gellan gum at various $Ca^{2+}$ concentrations and temperatures: (a) 2.0 mM, 43°C; (b) 2.5 mM, 32°C; (c) 3.5 mM, 37°C; (d) 3.0 mM, 32°C; and (e) 4.0 mM, 27°C ((a) and (b) are in the sol state and (d) and (e) are in the gel state; (c) corresponds to the state very near the gel point).

straight line (power–law dependence) over a wide delay time range. This sample was just like a very weak gel close to the gel point. This feature of the straight line means the power–law dependence holds, and agrees with the fractal nature of the gelling dendritic clusters having a very broad size distribution.

Figure 3 shows the temporal progress of the correlation function. With the increase of elapsed time, the profile of correlation function changes from that for the sol state to that for the gel state observed in Fig. 2. The time when the correlation function shows the most developed power–law behavior is regarded as the gelling time $t_g$ (Martin & Wilcoxon, 1988). Figure 4 shows the temporal progress of correlation function obtained by the multi-tau correlator, It is clear that the merging method gives essentially the same correlation function as by the multi-tau correlator. Correlation function showed a power–law relation with the slope of 0.3 at the elapsed time 800±30 min and this was considered to be the gelling time. The slope of 0.3 is quite comparable with the recent result of Lang & Burchard (1991).

Figure 5 shows the reciprocal plots of the scattered light intensity of 0.1% gellan gum of 2 mM $Ca^{2+}$ and 30.0°C at the intercourse of gelation as in Fig. 4. In this measurement, the sample cell was rotated, otherwise the scatter intensity did not give a smooth curve. With the lapse of time, scattered intensity gradually increases. The correlation length and the zero-angle scattered intensity were evaluated from the initial slope and the intercept. The gelling time was estimated from the correlation function measurements.

Figure 6 shows a double-logarithmic plot of correlation length as a function of the reduced time. The solid line has a slope of 0.89 for the exponent ν. On the other hand, Fig. 7 is a double-logarithmic plot of the reciprocal zero-angle scattered intensity. The slope of the solid line is 1.66. The zero-angle scattered intensity corre-

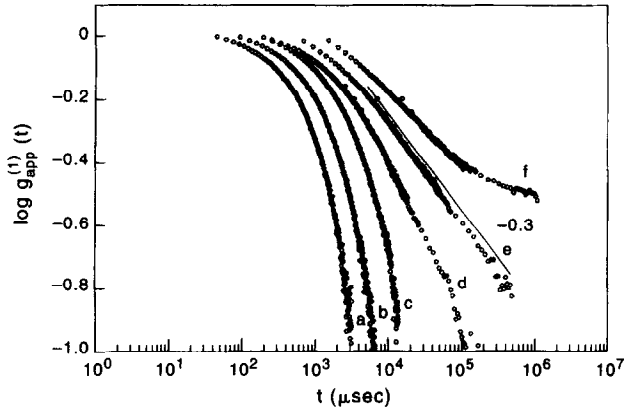


**Fig. 3.** Temporal progress of the time correlation function, $g^{(1)}{}_{app}(\tau)$, for 0.1% gellan gum in 3 mM $Ca^{2+}$ at 32.9°C. The elapsed time is (a) 0.9, (b) 120, (c) 210, (d) 290, (e) 452, and (f) 645 min. Around (e) a macroscopic network was formed and the slope of the curve is about 0.3.

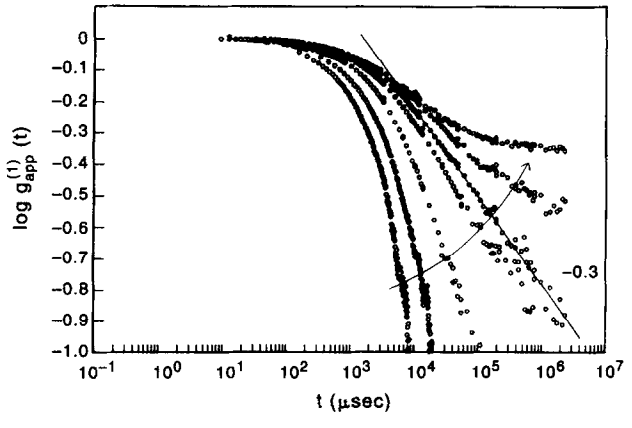


**Fig. 4.** Temporal progress of the time correlation function, $g^{(1)}{}_{app}(\tau)$ for 0.1% gellan gum in 2 mM $Ca^{2+}$ at 30.0°C. Correlation functions were obtained using the multi-tau correlator. The overall profiles are essentially the same as in Fig. 3. The slope of $g^{(1)}{}_{app}(\tau)$ where the macroscopic gelation occurs is about 0.3 and the gelling time was 800±30 min.

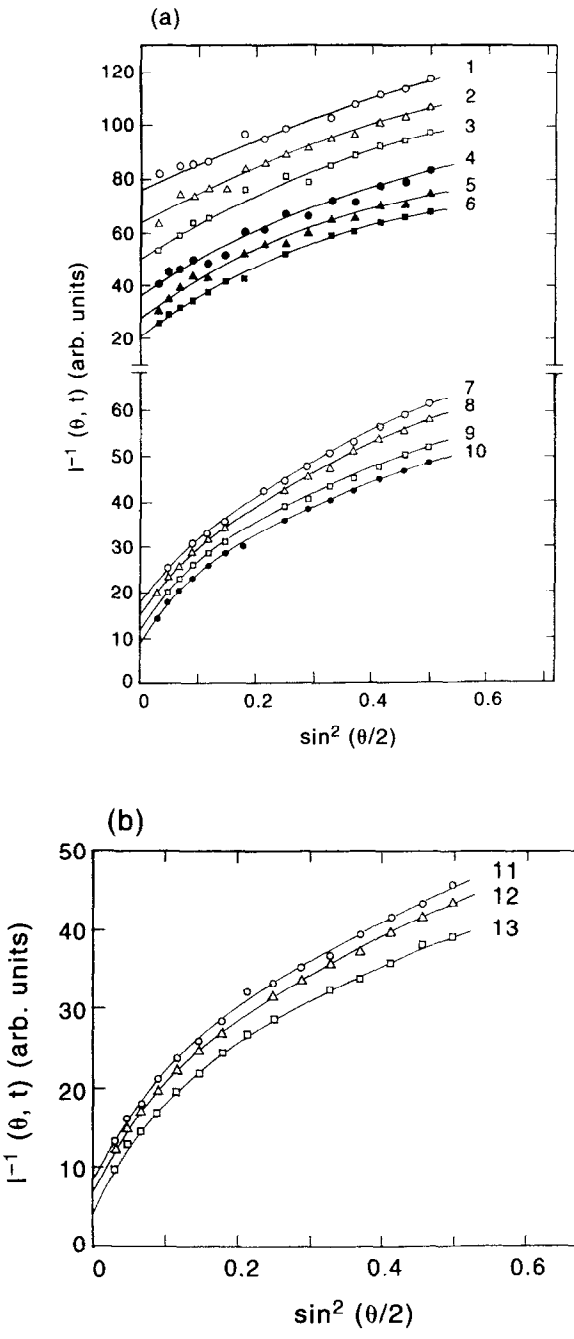


Fig. 5. Angular dependence of the scattered light intensity for 0.1% gellan gum in 2 mM $Ca^{2+}$ and at 30.0°C at various elapsed time. The elapsed times are 6, 54, 100, 166, 230, 277, 348, 392, 438, 491, 542, 583, and 621 min, respectively, for the curves from 1 to 13.

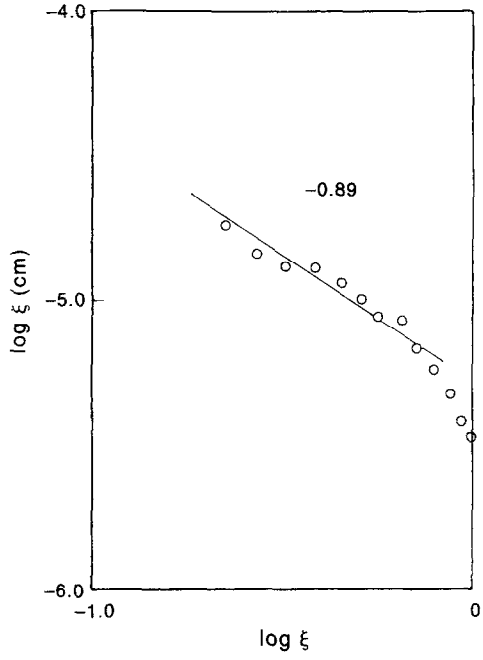


Fig. 6. Double-logarithmic plot of correlation length as a function of the reduced gelling time.

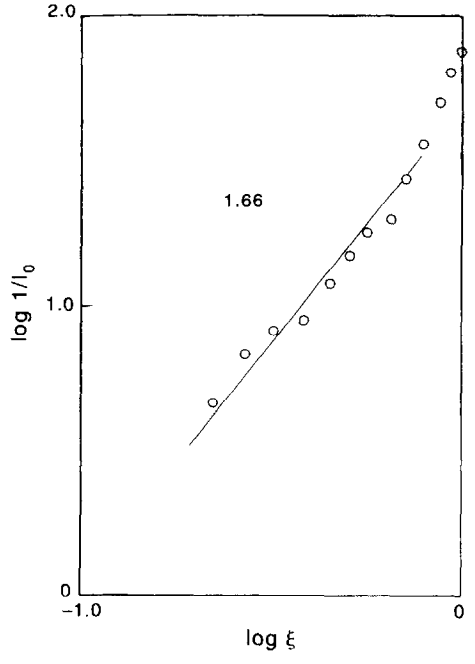


Fig. 7. Double-logarithmic plot of inverse zero-angle scattered intensity as a function of the reduced gelling time.

sponds to the weight averaged degree of polymerization of cluster mass and the exponent $\gamma$ is 1.66.

These two exponent values are compared with the predictions of the three-dimensional percolation model, in which $\nu$ and $\gamma$ are predicted to be 0.88 and 1.74, respectively (Stauffer *et al.*, 1982; Fang *et al.*, 1991). The agreement is good. Using the scaling relation of $d\nu = 2\beta + \gamma$, the resultant $\beta$ is 0.51 and is also in good agreement with the three-dimensional percolation model (0.45). These exponent values of $\nu$, $\gamma$ and $\beta$ differ distinctly from the classical mean field prediction ($\nu = 0.5$, $\gamma = 1.0$, $\beta = 1$).

According to Martin & Wilcoxon (1988), the following power-law of correlation function at the gel point was predicted as $g^{(1)}_{app}(\tau) \sim \tau^{-\Phi}$ with $\Phi = \beta/(\nu + k)$; $k$ being the exponent of the bulk viscosity, $\eta \sim \varepsilon^{-k}$. The exponent of the bulk viscosity, $k$, was evaluated to be 0.81 from $\Phi = 0.3$, $\beta = 0.51$, and $\nu = 0.89$. This exponent of viscosity, 0.81, is in good agreement with the result of

Adam *et al.*, 0.78 (Adam *et al.*, 1981), although the experimental verification of the viscosity exponent is still controversial (Fang *et al.*, 1991).

Our present results about the gelation process of gellan gum are well explained by the percolation model. This might be related to the very slow gelling reaction and the entangled situation even at the very dilute concentration of stiff gellan gum molecules and suggests that the gelling reaction does not cause changes of molecular assembled state of configuration in a very large scale.

In conclusion, the gelation process of gellan gum was well traced by the dynamic and static light scattering. The gel point was able to be determined well. The possible inhomegeneity introduced in the time course of gelation can be reduced by the cell rotation for the intensity measurements. The growth mechanism of gelation was explained by the percolation model, although the uncertainty of gelling time (about 30 min in the present work) still remains as a challenging problem.

## REFERENCES

Adam, M., Delsanti, M., Durand, D. & Hild Munch, J.P. (1981). Mechanical properties near gelation threshold, comparison with classical and 3D percolation theories. *Pure Appl. Chem,* **53,** 1489–1494.

Adam, M., Delsanti, M., Munch, J.P. & Durand, D. (1988). Dynamical studies of polymeric cluster solutions obtained near the gelation threshold, glasslike behavior. *Phys. Rev. Lett.,* **61,** 706–709.

Denkinger, P., Burchard, W. & Kunz, M. (1989). Light scattering from nonionic surfactants of the sugar–lipid hybrid type in aqueous solution. *J. Phys. Chem,* **93,** 1428–1434.

Dentini, M., Coviello, Y.W. & Crescenzi, V. (1988). Solution properties of extracellular microbial polysaccharide. 3. Light scattering form gellan and from the exocellular polysaccharide of *Rhizobium trifolii* (Strain TA-1) in the ordered state. *Macromolecules,* **21,** 3312–3320.

Fang, L., Brown, W. & Knoak, C. (1991). Dynamic light scattering study of the sol–gel transition. *Macromolecules,* **24,** 6839–6842.

Joosten, J.G.H., McCarthy, J.L. & Pusey, P.N. (1991). Dynamic and static light scattering by aqueous polyacrylamide gels. *Macromolecules,* **24,** 6690–6699.

Lang, P. & Burchard, W. (1991). Dynamic light scattering at the gel point. *Macromolecules,* **24,** 814–815.

Martin, J.M. & Wilcoxon, J.P. (1988). Critical dynamics of the sol–gel transition. *Phys. Rev. Lett.,* **61,** 373–376.

Milas, M., Shi, X. & Rinaudo, M. (1990). On the physicochemical properties of gellan gum. *Biopolymers,* **30,** 451–464.

Okamoto, T., Kubota, K. & Kuwahara, N. (1993). Light scattering study of gellan gum. *Food Hydrocoll.,* **7,** 363–371.

Pusey, P.N. & Megen, V.W. (1989). Dynamic light scattering by non-ergodic media. *Physica A,* **157,** 705–741.

Stauffer, D., Conglio, A. & Adam, M. (1982). Gelation and critical phenomena. *Adv. Polym. Sci.,* **44,** 103–158.

Stauffer, D. (1985). *Introduction to Percolation Theory.* Taylor & Francis, London.

Xue, J.-Z., Pines, D.J., Milner, S.T., Wu, X.-L. & Chaikin, P.M. (1992). Nonergodicity and light scattering from polymer gels. *Phys. Rev. A,* **46,** 6550–6563.